SPECIAL
Connecting the Tropics to the Polar Regions
COLLECTION

Composite Analysis of the Effects of ENSO Events on Antarctica

LEE J. WELHOUSE

Antarctic Meteorological Research Center, Space Science and Engineering Center, University of Wisconsin–Madison, Madison, Wisconsin

MATTHEW A. LAZZARA

Antarctic Meteorological Research Center, Space Science and Engineering Center, University of Wisconsin–Madison, and Department of Physical Sciences, School of Arts and Sciences, Madison Area Technical College, Madison, Wisconsin

LINDA M. KELLER, GREGORY J. TRIPOLI, AND MATTHEW H. HITCHMAN

Department of Atmospheric and Oceanic Sciences, University of Wisconsin–Madison, Madison, Wisconsin

(Manuscript received 1 February 2015, in final form 4 January 2016)

ABSTRACT

Previous investigations of the relationship between El Niño–Southern Oscillation (ENSO) and the Antarctic climate have focused on regions that are impacted by both El Niño and La Niña, which favors analysis over the Amundsen and Bellingshausen Seas (ABS). Here, 35 yr (1979–2013) of European Centre for Medium-Range Weather Forecasts interim reanalysis (ERA-Interim) data are analyzed to investigate the relationship between ENSO and Antarctica for each season using a compositing method that includes nine El Niño and nine La Niña periods. Composites of 2-m temperature (T_{2m}), sea level pressure (SLP), 500-hPa geopotential height, sea surface temperatures (SST), and 300-hPa geopotential height anomalies were calculated separately for El Niño minus neutral and La Niña minus neutral conditions, to provide an analysis of features associated with each phase of ENSO. These anomaly patterns can differ in important ways from El Niño minus La Niña composites, which may be expected from the geographical shift in tropical deep convection and associated pattern of planetary wave propagation into the Southern Hemisphere. The primary new result is the robust signal, during La Niña, of cooling over East Antarctica. This cooling is found from December to August. The link between the southern annular mode (SAM) and this cooling is explored. Both El Niño and La Niña experience the weakest signal during austral autumn. The peak signal for La Niña occurs during austral summer, while El Niño is found to peak during austral spring.

1. Introduction

This research focuses on the El Niño–Southern Oscillation (ENSO) signal found throughout Antarctic surface observations and reanalysis data. [For a more complete review of prior literature on interactions between ENSO and Antarctica see Turner (2004).] Understanding of ENSO, and its effects, has expanded substantially since it was initially investigated in depth. ENSO is now understood to be among the dominant modes of variability of both the atmosphere and ocean on decadal and subdecadal time scales. Its effects are found around the globe, rather than simply in the Pacific where it has its origin (Diaz and Markgraf 1992; Trenberth 1975a,b, 1976; Mo and White 1985). ENSO has been described as a coupled system linking an oceanic segment and an atmospheric segment, El Niño and the Southern Oscillation, respectively (Philander and Rasmusson 1985). The Southern Oscillation is measured using the surface pressure variations between the equatorial western and eastern Pacific, specifically between sites at Darwin, Australia, and Tahiti. The definition of El Niño for the oceanic Niño index (ONI) used predominantly in the literature, and throughout this work, is that of greater

Denotes Open Access content.

Corresponding author address: Lee J. Welhouse, Space Science and Engineering Center, 1225 West Dayton St., Madison, WI 53706.
E-mail: lee.welhouse@ssec.wisc.edu

DOI: 10.1175/JCLI-D-15-0108.1

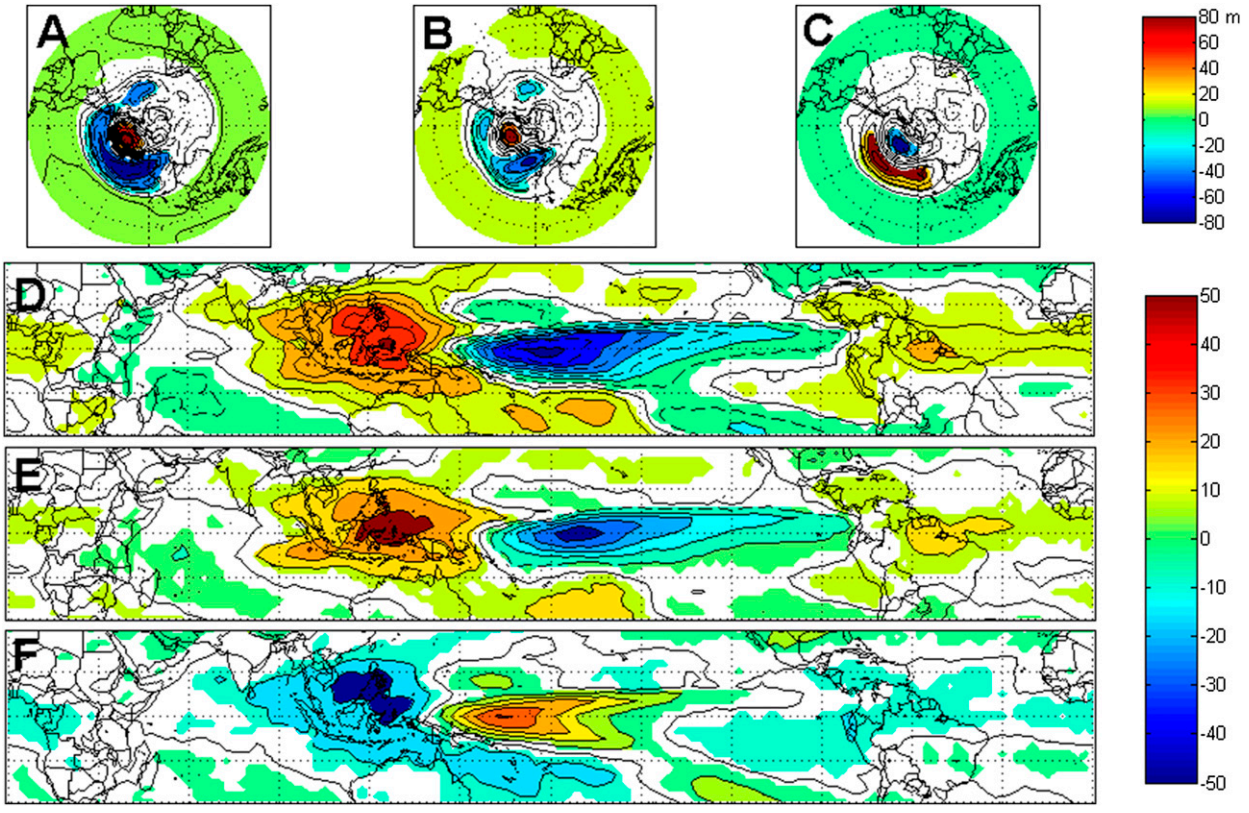

FIG. 1. The 500-hPa geopotential height anomalies (m) for the full year; regions with statistical significance exceeding the 95% confidence level represented by color filled regions: (a) El Niño − La Niña, (b) El Niño − neutral, and (c) La Niña − neutral. Tropical NOAA OLR values (W m^{-2}) for the full year with regions of statistical significance exceeding 95% confidence level represented by color-filled regions: (d) El Niño − La Niña, (e) El Niño − neutral, and (f) La Niña − neutral. Solid (dashed) contours indicate positive (negative) values.

than a 0.4°C anomaly from the mean of SSTs for 6 months or longer within the Niño-3.4 region (5°N–5°S, 150°–90°W) (NOAA/Climate Prediction Center 2015). Similarly, the definition of La Niña is a less than −0.4°C anomaly from the mean of SST for 6 months or longer within the Niño-3.4 region. These criteria indicate that El Niño conditions occur 31% of the time, La Niña conditions occur 23% of the time, and neutral events account for 56% of the time (Trenberth 1997). Recent work, by Jin and Kirtman (2009), suggests that the peak in Southern Hemisphere response leads the peak in tropical signatures of ENSO by approximately one season due to local seasonality in the tropical convection. This work will discuss timing of peak signals, and how these signals differ between El Niño events and La Niña events.

Considerable work has gone into determining mechanisms for transmission of a signal to explain the teleconnections found throughout the Southern Hemisphere. Hoskins and Karoly (1981) found that an area of deep convection near the equator can act to create Rossby waves, which then propagate to high latitudes. It was then indicated that these Rossby waves can have a further effect on mid- and high-latitude storm tracks in turn, allowing larger effects at high latitudes from smaller changes in tropical SSTs (Held et al. 1989). Such wave trains are known as the Pacific–North American (PNA) pattern in the Northern Hemisphere and the Pacific–South American (PSA) pattern in the Southern Hemisphere (Karoly 1989). Specifically for this work, the important PSA pattern is the PSA-1 pattern found in Karoly (1989), which is largely associated with ENSO variability in tropical convection. Though there was initially less evidence to support this designation, further investigation into the PSA pattern has indicated that it has effects throughout the Southern Hemisphere (Harangozo 2000; Mo and Higgins 1998). Often ENSO teleconnections in the region have been analyzed in a largely symmetric manner, through composites of El Niño − La Niña (Fig. 1a) and spatial correlation maps that incorporate both phases of ENSO. Symmetry assumes El Niño and La Niña will have equal and opposite impacts in generally similar regions, which is generally a good assumption as seen in Figs. 1b and 1c. There are

subtle differences in location with La Niña events shifted toward the Ross Ice Shelf region stretching into East Antarctica (Fig. 1c), while El Niño shows a signal closer to the peninsula (Fig. 1b) stretching into the Ross Ice Shelf. We explore these subtle differences on seasonal time scales throughout this work. Recent research indicates the presence of significant nonlinearities, and asymmetries in tropical regions between phases of ENSO (Frauen et al. 2014). These differences warrant an exploration of how the phases impact the associated teleconnections. Because of the prior symmetric view, the literature (Turner 2004) has predominantly focused on the Amundsen–Bellingshausen Sea (ABS) region and much of West Antarctica. This is due to the ABS and West Antarctica being a region where El Niño and La Niña have opposite impacts, and it is the primary region of impact related to Rossby wave trains associated with the PSA. Regions where a single phase of ENSO impact, such as East Antarctica during La Niña events, will be largely ignored by these methods due to statistically significant patterns being more difficult to find (Houseago-Stokes and McGregor 2000). Surface area temperature signals throughout this region have been commented on in prior literature (Schneider et al. 2012) as being potentially related to a coupling of southern annular mode (SAM) and ENSO during austral summer. Other mechanisms for variation of teleconnections seen at high southern latitudes are currently being explored and include interactions with the Indian Ocean dipole (IOD), SAM, and variability of tropical convection outside of the tropical Pacific (Clem and Fogt 2013; Li et al. 2015; Wilson et al. 2014). Of particular interest for this study are investigations into the timing and extent of teleconnection patterns as well as asymmetries in the form of distinctions between El Niño and La Niña signals. This study explores the regions of these distinctions in depth in an attempt to categorize the impact ENSO has on Antarctica during each phase of ENSO as well as, where viable, to separate the impact of ENSO from that of the SAM.

2. Data and methods

Numerous reanalysis datasets have been analyzed to ensure broad agreement throughout both newer and older datasets. Though it is beyond the scope of this study to fully validate reanalyses, these datasets have been compared with various Automatic Weather Stations (AWS) throughout Antarctica to ensure accuracy within the regions of important signal. There was good agreement found in all regions discussed over the time period, with high correlation to surface temperature and pressure observation data (not shown). While biases were found in the reanalysis they were relatively consistent throughout the period explored. More information on these stations can be found in Lazzara et al. (2012). Validation of older reanalyses indicates they are sufficiently accurate, during the time period, for the purposes of this study (Bromwich and Fogt 2004; Yu et al. 2010). This section describes the primary dataset utilized as well as the methodologies used to explore the data. Of particular interest is the European Centre for Medium-Range Weather Forecasts (ECMWF) interim reanalysis (ERA-Interim, 1979–2013) (Dee et al. 2011), as it has been shown to be the best reanalysis currently available (Bracegirdle and Marshall 2012; Jones and Lister 2015). The Climate Forecast System Reanalysis (CFSR, 1979–2011), and the 40-yr ECMWF Re-Analysis (ERA-40, 1979–2002) have also been analyzed with the methods described in this study, and there is large agreement between the reanalysis products with regard to the signals discussed, though these products capture fewer events, and are of lower quality. Hence, results are shown only for ERA-Interim.

a. *ERA-Interim*

While the ERA-Interim dataset will be used in this analysis, the product is not without potential spurious trends. For that reason, the data have been compared with surface observational data and found to be in good agreement (not shown; Bracegirdle and Marshall 2012). The tropical outgoing longwave radiation (OLR) in the convectively active regions of the tropics is limited in accuracy (Itterly and Taylor 2014), so the National Oceanic and Atmospheric Administration (NOAA) OLR has been used as a proxy for tropical convection. Further, efforts have been made to analyze detrended data, and limited impact was found when compared to nondetrended data for this analysis. This, at first, seems contradictory given the importance of the SAM trend and the impact it has on ENSO signals, but this emphasizes the difficulty of separating the SAM and ENSO signals. The ERA-Interim has a resolution of 0.75° × 0.75° and extends from January 1979 to the present. For the purposes of this analysis, the time period analyzed was January 1979–December 2013. The ONI consists of 3-month averages of SST over the Niño-3.4 region. Because of this, the values from the reanalysis were formed into 3-month means for the composites. Surface pressure (Fig. 4), SST (Fig. 6), 2-m temperature (T_{2m}; Fig. 5), 500-hPa geopotential heights (Fig. 3), and 300-hPa geopotential heights (Fig. 2) have been evaluated.

b. *Composite methods*

There are a number of steps necessary to form composites of any given phenomenon. The first step is choosing a means to define events for compositing. In

TABLE 1. List of El Niño events during 1979–2014 with the beginning and end point for each event.

El Niño events	La Niña events
Apr 1982–Jul 1983	Aug 1983–Feb 1984
Jul 1986–Mar 1988	Sep 1984–Oct 1985
Apr 1991–Jul 1992	Apr 1988–Jun 1989
Aug 1994–Apr 1995	Aug 1996–Apr 1997
Apr 1997–May 1998	Jun 1998–Apr 2001
Apr 2002–Mar 2003	Oct 2005–Apr 2006
Jun 2004–Feb 2005	Jul 2006–Jul 2007
Aug 2006–Feb 2007	Jun 2010–May 2011
Jun 2009–May 2010	Mar 2011–Apr 2012

prior work on ENSO composite analysis, generally the positive basis was used to describe El Niño events, and the negative basis was used to describe La Niña events (Karoly 1989; Turner 2004). More recent studies (Fogt et al. 2011; Fogt and Bromwich 2006) have analyzed composites of separate phases, which are particularly useful in determining the distinct features of each phase. This study has used the definition of events described by the ONI to assign the events and nonevents. Specifically, El Niño or La Niña events are compared with non-ENSO events. After the events are chosen, they are averaged. These averaged events are subtracted from the average of the nonevents to form the composite. Finally, statistical significance is determined by using a two-tailed Student's t test, and for the cases evaluated, the confidence interval has been set at 0.95 and is denoted with colored shading.

c. Southern annular mode

Previous studies (Fogt et al. 2011; Fogt and Bromwich 2006; Schneider et al. 2012; Ciasto and Thompson 2008; L'Heureux and Thompson 2006) have explored the interactions between ENSO and SAM, finding coupling between the phenomena with strong linear interactions during the austral summer. Composite analysis finds, as in prior literature (Schneider et al. 2012), a striking similarity between the La Niña T_{2m} and the SAM T_{2m} signals. In the interest of exploring the signal without the SAM, the regression of the SAM has been removed from the T_{2m} during austral summers of both El Niño and La Niña events. The December–February (DJF) period was chosen as this is the period that shows a strong trend toward positive SAM, while other seasons have a less explicit impact from SAM.

3. Composite analysis and results

To ensure this analysis is not the result of just one reanalysis product, or spurious trends within a single product, comparison between multiple products is performed (not shown). While only the ERA-Interim is shown, the other reanalysis products analyzed all agree on the findings this work discusses, despite covering shorter periods of time or being from earlier generations of reanalyses. Further, more effort goes into discussing the impacts of La Niña events as many of the impacts of El Niño have already been categorized in previous literature (Fogt et al. 2011; Turner 2004; Fogt and Bromwich 2006, Clem and Fogt 2013) as they impact the ABS region. This region, while of great importance when discussing ENSO teleconnections in Antarctica, is not the only area of interest. All areas discussed achieve a confidence interval of 0.95 unless otherwise indicated. As it is of general importance to still compare El Niño and La Niña, the following figures show both El Niño [panels (a)–(d)] and La Niña events [panels (e)–(h)].

a. El Niño

El Niño events generally account for approximately 31% of the SST conditions, and there have been nine events during 1979–2014 (Table 1). Prior work indicates an expected ABS higher pressure area (Turner 2004). Of primary interest in this work is the seasonality of the signal seen in the ABS region. Seasonality of ENSO events has been explored in Schneider et al. (2012), finding limited interactions in the Antarctic Peninsula during DJF with a peak during September–November (SON). Schneider et al. (2012) explored ENSO with techniques predominantly focused on both phases of ENSO, which may explain some of the disparities with this work.

When analyzing the 300- and 500-hPa geopotential height fields (Figs. 2 and 3) along with the SLP (Fig. 4) we find an expected barotropic atmosphere during June–August (JJA) (Figs. 2c, 3c, and 4c) and SON (Figs. 2d, 3d, and 4d) as well as the strongest impact throughout the ABS region. This lines up well with prior literature (Schneider et al. 2012; Jin and Kirtman 2009; Jin and Kirtman 2010). This signal takes the form of a positive geopotential height anomaly in the ABS region. A negative geopotential height anomaly throughout the Weddell Sea region also appears in JJA at upper levels (Figs. 2c and 3c), whereas a positive anomaly is found throughout the ABS region and the Weddell Sea region during DJF (Figs. 2a and 3a). This DJF signal is particularly different than all other periods for El Niño events. This is due to a change in the underlying mechanisms of the teleconnection (Schneider et al. 2012; L'Heureux and Thompson 2006). Schneider et al. (2012) found that during DJF periods, the ENSO teleconnection related to a projection of ENSO variability onto the SAM could explain this departure, as the variability of SAM during this period could significantly impact the teleconnection within the area (Fogt et al. 2011).

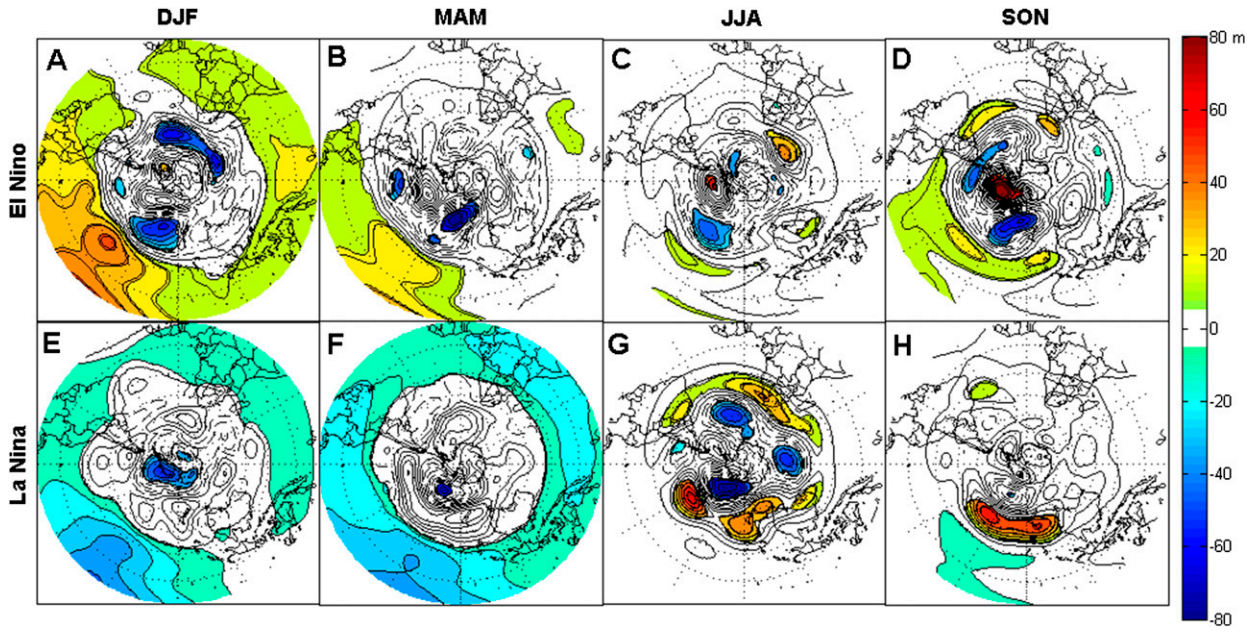

FIG. 2. The 300-hPa geopotential heights (contours every 8 m). Solid (dashed) contours indicate positive (negative) values and color-filled regions indicate statistical significance exceeding the 95% confidence interval: El Niño is neutral during (a) DJF, (b) MAM, (c) JJA, and (d) SON; (e)–(h) As in (a)–(d), but for La Niña.

Winds associated with these changes in geopotential heights, through advection, act to change temperatures throughout the ABS region (Figs. 5c,d). Specifically, increased temperatures are noted in the Ross Ice Shelf region as well as the ABS region during these periods, associated with warm moist air being transported southward, while cooler temperatures are noted throughout the Antarctic Peninsula and Weddell Sea region, associated with cooler air being drawn north. Further, analyzing SST (Figs. 6c,d) we note that the peak temperature anomalies shifted to the central Pacific. SON has two separate regions of maximum temperature—one being in the central Pacific and the other being in the eastern Pacific (Fig. 6d). When comparing SON and JJA, it is notable that SON has the stronger tropical signal, which coincides with the stronger signal at high latitudes.

During the March–May (MAM) and DJF time periods, signals are different than what is typically associated with ENSO (Fig. 1). In MAM (Figs. 2b, 3b, and 4b), the signal is largely absent from a statistically significant standpoint and is weaker, as well as shifted slightly north from a standpoint of spatial patterns. Despite this, surface area temperature signals associated with an El Niño during these months exist (Fig. 5b), with cooling found in the Antarctic Peninsula. In the tropics, we note that the SST (Fig. 6b) shows the strongest temperature anomaly shifted to the eastern Pacific just off the coast of South America, which is considerably different from other periods.

During the DJF period, there are considerable differences in the significance of signals seen at various geopotential heights, with a significant positive geopotential height anomaly seen at upper levels in the Weddell Sea region, and a nonstatistically significant positive geopotential height anomaly in the ABS region shifted toward the Ross Ice Shelf (Figs. 2a and 3a). At the surface a high pressure anomaly is found throughout the ABS region stretching toward the Ross Ice Shelf (Fig. 4a), though this is different from the normal signal associated with El Niño as it is shifted toward the Ross Ice Shelf. This has little impact on T_{2m} with a small region of cooling in the southern Ross Ice Shelf and small warming in the Antarctic Peninsula and the ABS region off the coast of West Antarctica (Fig. 5a). Within the SST (Fig. 6a) we note the strongest anomalies during this season, but as previously mentioned, during DJF the signal lines up more with a projection of ENSO variability onto the SAM, or as out of phase with the SAM (Schneider et al. 2012; Fogt and Bromwich 2006). In other words, due to the positive trend in SAM the El Niño signal is weakened substantially during this period.

b. La Niña

There have been approximately 12 La Niña years from 1979 to 2014, though many of these are weak and due to prolonged La Niña conditions (Table 1). While analysis of El Niño events generally provided the expected result associated with ENSO events—a distinct

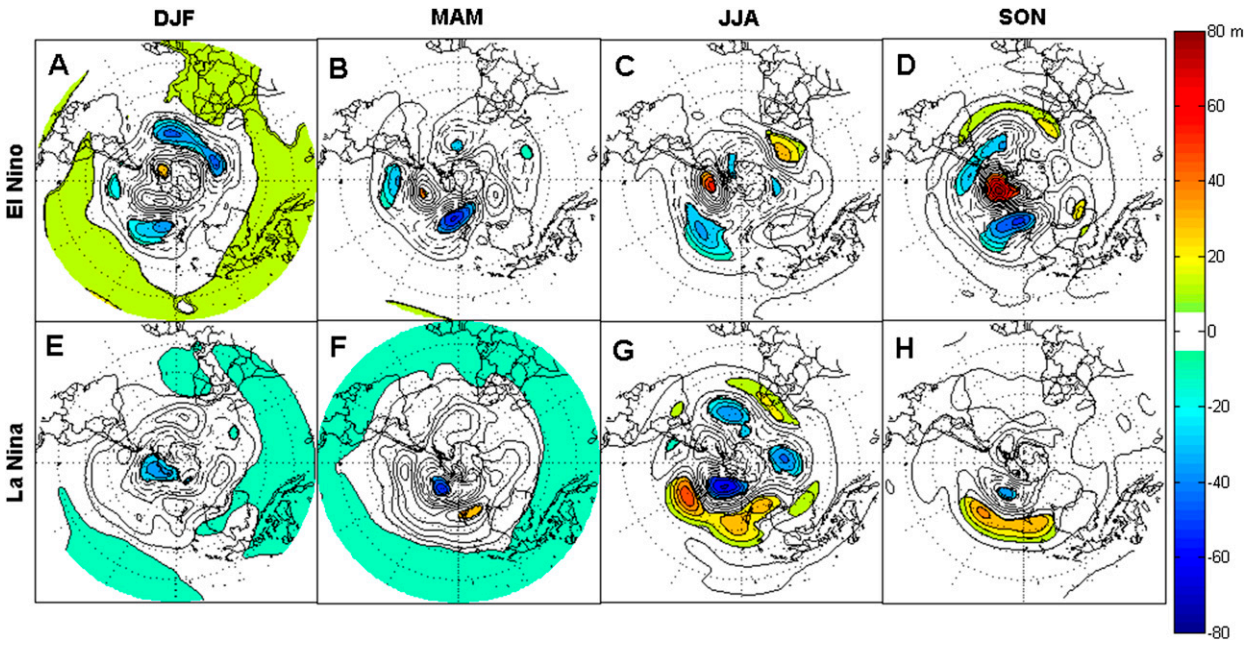

FIG. 3. As in Fig. 2, but for 500-hPa geopotential heights.

signal in the ABS region (Turner 2004) or no distinct signal—analysis of La Niña events provides a quite different picture. A more symmetric view of ENSO signals would indicate similar areas of effect with opposing signals, so El Niño having a distinct positive geopotential height anomaly in the ABS region would require La Niña to have a negative geopotential height anomaly in the same region. While this signal is found in some seasons, it is shifted toward the Ross Ice Shelf region and additional signals are found in other regions.

The La Niña signal of a negative geopotential height anomaly (Figs. 2 and 3), low pressure anomalies (Fig. 4), and T_{2m} (Fig. 5) anomalies associated with advection, in the ABS region is readily apparent throughout the

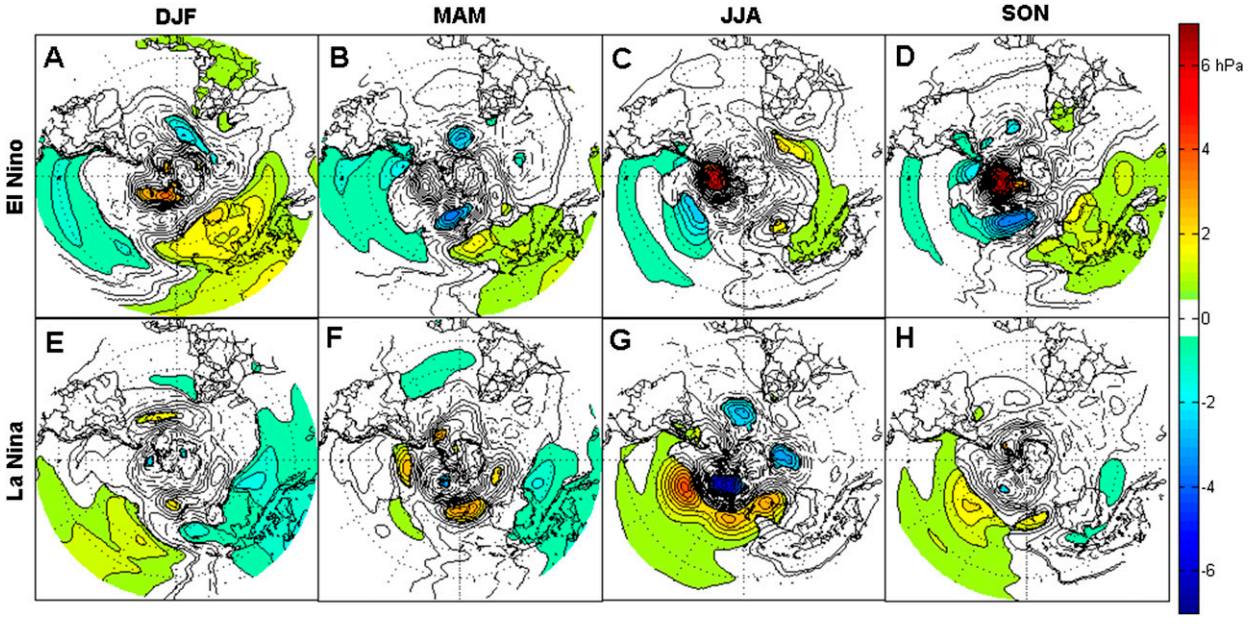

FIG. 4. As in Fig. 2, but for sea level pressure with a contour interval of 0.6 hPa.

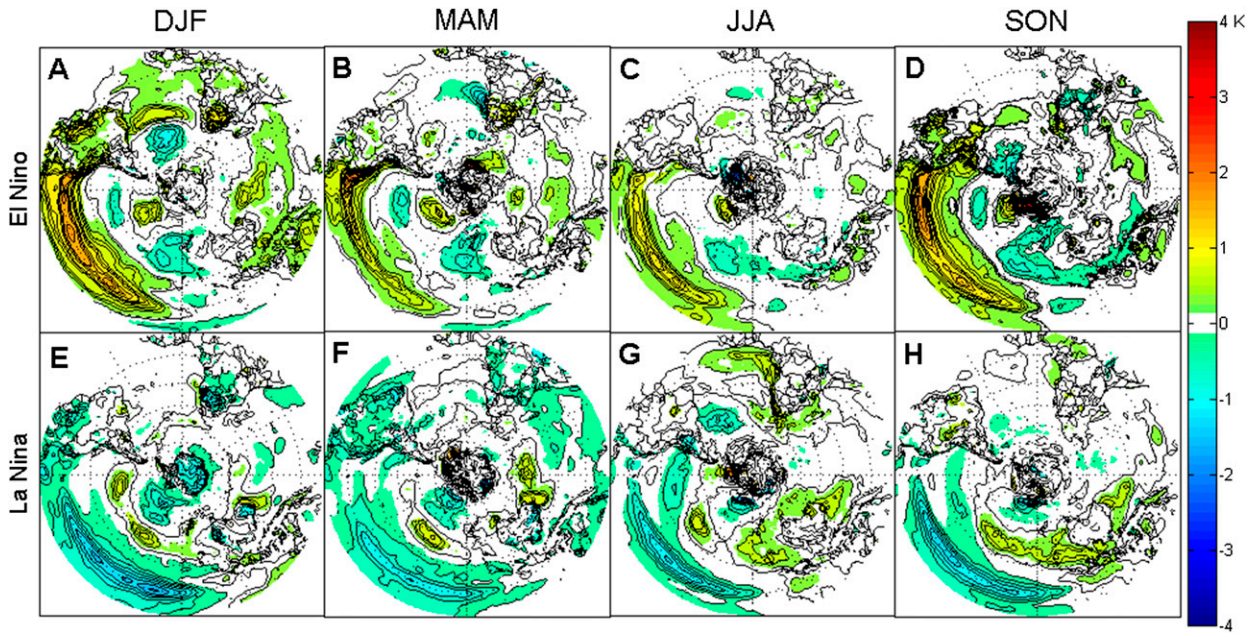

FIG. 5. As in Fig. 2, but for T_{2m} temperatures in kelvin with a contour interval of 0.2 K.

seasons, with variations primarily seen in the strength of the signal and how far south it extends. The expected signal consists of negative geopotential height anomalies in the Ross Sea and ABS regions, with warming seen in the Antarctic Peninsula and cooling of the Ross Sea. While this is seen in all of the seasons, the signal is shifted toward the Ross Ice Shelf in all seasons at upper levels (Figs. 2 and 3). Also notably, during DJF (Figs. 2e and 3e), MAM (Figs. 2f and 3f), and JJA (Figs. 2g and 3g) the upper-level negative geopotential height anomalies stretch into East Antarctica, though this is only statistically significant during DJF. The months with the most prominent signal for the El Niño were shown to be JJA and SON, while for La Niña the seasons with the most

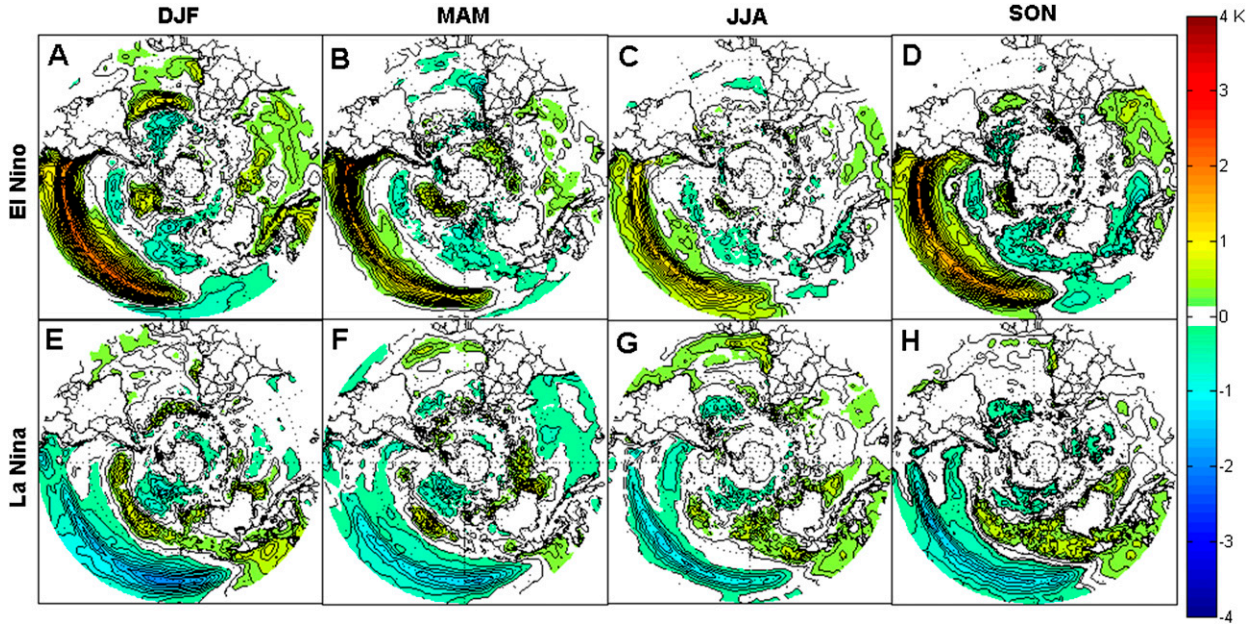

FIG. 6. As in Fig. 2, but for sea surface temperatures with a contour interval of 0.2 K.

prominent signal are JJA and DJF. For La Niña events, the SON signal is considerably weaker and shifted north away from Antarctica (Figs. 2g and 3g). This results in considerably different temperature patterns with no impact in the peninsula, and warming found in the northern portion of the Ross Ice Shelf (Fig. 5g). MAM is relatively weak for both phases though La Niña shows a more robust signal than El Niño during this season. This may be due to asymmetries in the duration of events (Okumura and Deser 2010). Considerable variations of these teleconnections exist throughout the atmosphere depending largely on seasonality. Because of the relatively barotropic nature of the high southern latitude atmosphere, all levels show approximately the same patterns in geopotential height and pressure anomalies, though significance varies a great deal. Despite the comparatively small signal during MAM and SON, there are consistent signals at each layer examined that line up with the patterns associated with ENSO signals, slightly shifted toward the Ross Ice Shelf (Figs. 2f,g; 3f,g; and 4f,g).

Despite the lack of statistically significant SLP anomalies during DJF, the T_{2m} anomalies (Fig. 5e) are the widest spread during these months, with cooling in West Antarctica and the adjacent ocean regions, and warming in the Antarctic Peninsula. The cooling in West Antarctica, and warming in the peninsula is expected due to advection associated with statistically significant geopotential height changes seen throughout the upper atmosphere (Figs. 2e and 3e) as well as pressure field changes seen at the surface (Fig. 4e). Also, extensive cooling is seen throughout East Antarctica, and in previous literature (Schneider et al. 2012; Ciasto and Thompson 2008; L'Heureux and Thompson 2006) this has been linked to a coupling of SAM and ENSO, with La Niña being in phase with positive SAM. Given the trend toward positive values of SAM, particularly in summer (Marshall 2003) and the interaction between positive SAM and La Niña events, the teleconnection signal is amplified during this season. The presence of temperature signals throughout East Antarctica, and specifically in coastal Wilkes Land, during most seasons (Figs. 5e–g) indicates a connection with ENSO. The small region of cooling in Wilkes Land seems directly attributable to ENSO, as it persists through multiple seasons, while the cooling seen throughout the rest of East Antarctica in DJF (Fig. 5e) is likely due SAM, and particularly visible due to the trend toward positive amplifying the cold anomalies.

In analyzing the SST (Fig. 6) a number of patterns become evident. The pattern of cold water extending farther into the western Pacific is notable during all seasons, as expected with La Niña cold tongue expansion. DJF (Fig. 6e) and MAM (Fig. 6f) show the coldest temperature anomalies farthest to the west, while JJA (Fig. 6g) and SON (Fig. 6h) show more central Pacific cooling. This cooling acts to shut down central and eastern Pacific convection seen during El Niño events and shift convection into the western Pacific near Indonesia and Australia where small warm anomalies are found. These features line up with the extent of cooling and negative geopotential height anomalies seen in East Antarctica, with DJF and MAM (Figs. 5e and 5f) showing the most cooling, while JJA and SON (Figs. 5g and 5h) show less or no cooling. A relatively stronger pattern of warm anomalies is found south of the western edge of the cold tongue during SON (Fig. 6g). This slightly south and eastward displaced warm water, and associated convection, could indicate the shifted pattern in the SON La Niña teleconnection.

The cooling in East Antarctica (Figs. 5e–g) is found under a region that has shown a modest signal associated with the PSA-1 pattern (Mo and Higgins 1998) and is associated with changes in tropical convection. The westward shift, in comparison with non-ENSO years, in tropical convection (Deser and Wallace 1990) and south and westward shift in the South Pacific convergence zone (SPCZ) (Folland et al. 2002) provide a physical mechanism for this cooling as this shift in convection also acts to shift the source of the Rossby wave train westward. We have explored these changes in convection with the methods described in this paper, and found good agreement with Deser and Wallace (1990) and Folland et al. (2002) (Figs. 1d–f). This westward shift, when coupled with the downstream high topography of the East Antarctic plateau acting to block the propagation of the teleconnection explains both the cooling seen in East Antarctica, as well as the relatively weaker impacts seen during La Niña in general. More specifically the teleconnection location is shifted to East Antarctica resulting in lower geopotential height anomalies, and changes in wind patterns resulting in the cooling found.

c. *Southern annular mode*

It is of considerable interest to attempt to find a method to tease apart the coupled signals of SAM and ENSO. Unfortunately, a lack of sufficient events of negative and negative SAM events during La Niña and El Niño events, respectively, makes direct composite analysis ill-suited to this task. A viable alternative to explore the separate signals is to remove the regression of the SAM from the composite of ENSO events. Because of the interconnected nature of SAM and ENSO, this method will be particularly conservative in estimating the impact of ENSO. This is due to the fact that the removal takes out a substantial portion of the signal associated with SAM, as well as the signal associated with interactions between ENSO and SAM, and

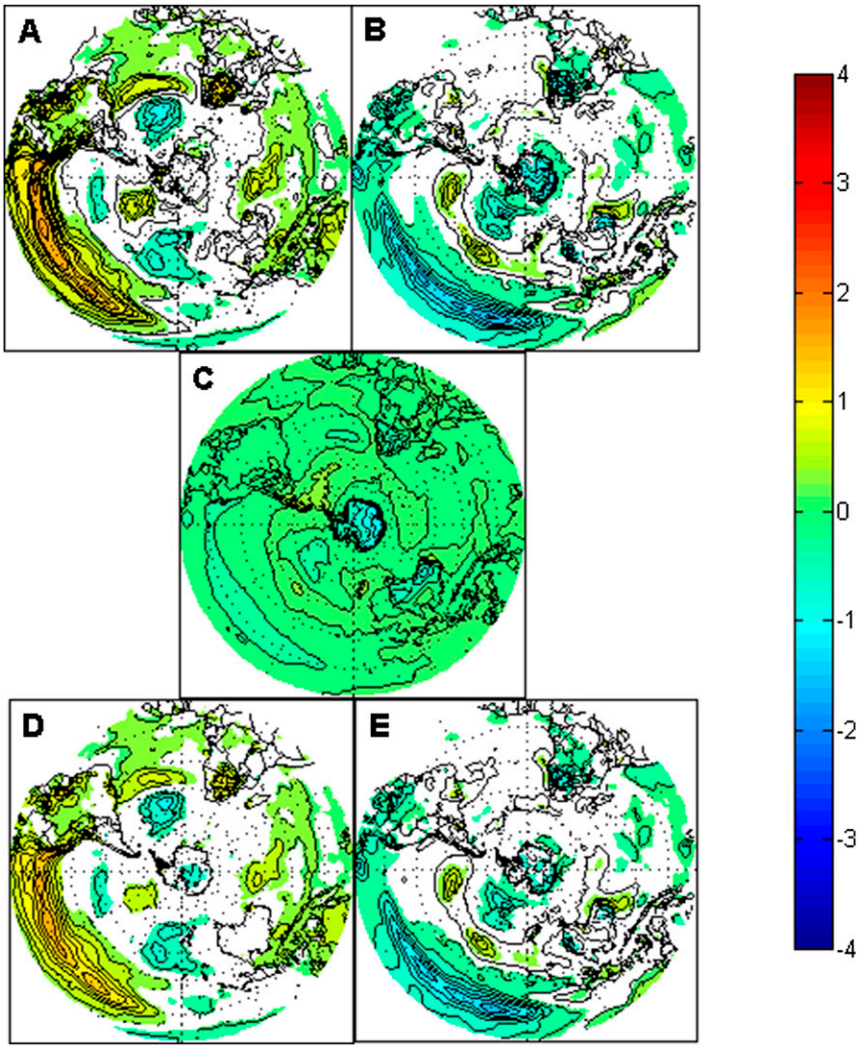

FIG. 7. A comparison of La Niña and El Niño composites of 2-m temperature before and after the removal of SAM regression with a contour interval of 0.2 K: (a),(b) El Niño and La Niña are neutral during DJF, respectively; (c) SAM regressed onto T_{2m} field with values being the response in kelvin per SAM index. (d),(e) El Niño and La Niña 2-m temperature after the SAM regression have been removed, respectively. In (a)–(d), color-filled regions indicate statistical significance exceeding the 95% confidence interval.

the variability of ENSO captured within the SAM index. During DJF, there is strong interaction between ENSO and SAM signals causing a significant change in the patterns seen as shown throughout this paper as well as in prior literature (Schneider et al. 2012; Fogt et al. 2011). Given this, it is likely that a portion of the ENSO signal is removed with this technique. Despite all these caveats, this provides a somewhat useful perspective of what La Niña and El Niño might look like in the absence of trends in SAM.

During La Niña the remaining statistically significant signal consists of a small region of negative temperature anomaly along the East Antarctic coastal region, as well as negative temperature anomalies throughout the Ross Sea and ABS regions, a slight warming of the Antarctic Peninsula, and a small region of cooling within the East Antarctic plateau (Fig. 7e). The placement of the East Antarctic temperature anomaly is similar to the anomalies seen in other seasons (MAM and JJA) (Figs. 5f and 5g). The temperature signals throughout the Ross Sea and ABS region remain as these regions are not associated with SAM, and would be associated with advection caused by a negative geopotential height anomaly in the Ross Sea and ABS regions. The cooling in East Antarctica lines up with a westward shift in teleconnections as discussed earlier.

During El Niño (Fig. 7d) the relatively small regions of statistically significant warming seen in the Antarctic Peninsula have expanded, as has the cooling seen in the Ross Ice Shelf, with some shift into East Antarctica. This signal so far afield from the usual region of West Antarctica, and the Antarctic Peninsula is a bit unexpected, but is not unrealistic given the significantly abnormal upper-level patterns seen during DJF in El Niño events (Figs. 2a and 3a). This expansion of temperature signals makes sense, as positive SAM is expected to weaken the El Niño teleconnection (Fogt et al. 2011), though the location of the anomalies remains abnormal when compared with other seasons of El Niño. Further exploration into the dynamics of El Niño teleconnections during this season is an area of growing study, which is unfortunately outside the capabilities of the techniques used within this analysis.

4. Discussion

In earlier ENSO studies, composite analyses were performed using El Niño − La Niña (e.g., Mo and Higgins 1998; Turner 2004). This technique emphasizes regions of common but opposite effect allowing for statistical significance to more easily be achieved within these regions. At the same time it discounts asymmetries in the form of common regions of similar effect as seen during DJF warming in the peninsula during both phases (Figs. 5a and 5e), regions that see effects in one phase of ENSO events only as seen in the East Antarctic cooling during La Niña events (Figs. 5e–g), and makes differences in timing between the two phases difficult to determine. By separating the composites to view El Niño and La Niña as distinct events, these features become evident.

The general signal associated with ENSO teleconnections within the Antarctic seems to be primarily associated with El Niño events, and some seasons during La Niña events. Further, the El Niño aspect of the signal is shifted toward the Antarctic Peninsula, while La Niña events are shifted toward the Ross Ice Shelf, and in some seasons seems to be split by the Transantarctic Mountains showing clear signals within East Antarctica as well as signals within the ABS region though shifted toward the Ross Ice Shelf. This ENSO signal has been shown to have a demonstrable effect on Antarctic T_{2m} and mean sea level pressures. More specifically, during El Niño events, it generally acts to warm West Antarctica and cool the Antarctic Peninsula.

There is also a clear signal associated with La Niña events during DJF and JJA. Both of these seasons are characterized, at upper levels, by negative geopotential height anomalies that stretch toward the Transantarctic Mountains, and during DJF the signal seems to be split by this terrain feature as well as having a far more poleward signal. Fogt and Bromwich (2006) indicate that a strong coupling exists between the SAM and ENSO such that a positive (negative) SAM indicates a stronger La Niña (El Niño) signal seen at high latitudes. As the SAM has been trending positive most strongly in austral summer, there is a prominent reason to expect a more robust signal during DJF for La Niña and a weaker signal for El Niño (Marshall 2003).

An initial goal of this analysis was to determine what signal, if any, associated with the specific phases of ENSO events could be found at the surface in Antarctica, and it has led to a number of general findings. During this time period, El Niño events can be categorized as having an effect shifted toward the Antarctic Peninsula and Weddell Sea, with some impacts in West Antarctica and the Ross Ice Shelf. La Niña events can be categorized as having impacts shifted toward the Ross Ice Shelf, with impacts in West Antarctica, the Ross Ice Shelf, and East Antarctica. El Niño generally has an impact of cooling throughout the peninsula and adjacent ocean, with inconsistent warming seen in coastal West Antarctica and the Ross Ice Shelf predominantly during SON. These features make sense from a physical standpoint as shifts in the regions of convection depends on both seasonality, as well as phase of ENSO, with El Niño events shifting convection eastward and the SPCZ shifted north and east, and La Niña events shifting convection westward with the SPCZ shifted south and west.

Prior to this study, La Niña events were expected to affect similar regions as El Niño events, but this analysis shows that East Antarctica experiences large-scale cooling during La Niña events, which has been linked to interactions with SAM. Further exploration of this East Antarctic cooling indicates a small portion is less dependent on interactions with SAM, and is a region associated with PSA-1 pattern teleconnections associated with shifts in convection largely associated with ENSO. This East Antarctic signal is predominantly associated with La Niña events. While signals within this region have existed in prior literature they have often gone undiscussed, or are not linked to La Niña. They are potentially associated with warm water being more concentrated near Indonesia during La Niña events, modulating ascending air and inciting Rossby waves as discussed by Lachlan-Cope and Connolley (2006), though more analysis is necessary to confirm this. Further, there are strong seasonal aspects to the temperature impacts throughout West Antarctica with regions near the peninsula experiencing warming during JJA, and other regions experiencing cooling during DJF, with these inconsistent patterns being undetectable in analysis of annually averaged teleconnection patterns.

5. Conclusions

Composite analysis has been shown to be an effective means of analyzing ENSO effects at high latitudes, and the new method of using nonevents as one portion of the comparison allows for differences between different phases of ENSO, El Niño, and La Niña to be distinguished. It must still be acknowledged that a relatively few number of events have been analyzed due to the quality of reanalysis data for the Southern Hemisphere prior to 1979 being in question (Bromwich and Fogt 2004). Despite the small number of events, a number of conclusions can be drawn from the composite analyses performed. As expected, the ABS region remains the primary location of strong teleconnections, with El Niño generally indicating a positive geopotential height anomaly extending toward the Antarctic Peninsula and La Niña indicating a negative geopotential height anomaly extending toward the Ross Ice Shelf. There also seems to be greater seasonal variance in the signal during La Niña events than El Niño events. This is indicated by the consistent late austral summer effect in East Antarctica seen both in the surface area temperatures, as well as throughout the upper atmosphere. This East Antarctica signal warrants further exploration for mechanisms of changes in the location of teleconnections, as it has largely been viewed as an interaction of ENSO and SAM, which may not fully explain the interactions. The seasonality of both phases of ENSO, particularly the breakdown of the signal during peak ENSO months also warrants further exploration as prior studies indicate that a lack of a signal in the Antarctic Peninsula during DJF is paradoxical (Schneider et al. 2012), but based on this analysis it seems both phases are having a similar impact on warming.

Acknowledgments. This material is based upon work supported by the National Science Foundation Grants ANT-1245663, ANT- 0944018, and AGS-1256215. ECMWF ERA-40 and ERA-Interim data used in this study have been obtained from the ECMWF data server. The CFSR and NCEP–NCAR reanalysis data were developed by NOAA's National Centers for Environmental Prediction (NCEP). The data for this study are from the Research Data Archive (RDA), which is maintained by the Computational and Information Systems Laboratory (CISL) at the National Center for Atmospheric Research (NCAR). The National Center for Atmospheric Research is sponsored by the National Science Foundation. The original data are available from the RDA (http://rda.ucar.edu) in dataset number ds093.2. Uninterpolated OLR data were provided by the NOAA/OAR/ESRL PSD, Boulder, Colorado, from their web site at http://www.esrl.noaa.gov/psd/. The authors thank Dan Vimont of the Atmospheric and Oceanic Sciences Department at the University of Wisconsin–Madison, and Ryan Fogt of the Department of Geography at The Ohio State University, for their assistance in methods for analyzing interactions between ENSO and SAM. The authors would also like to thank David Bromwich of The Ohio State University for organizing this special issue, as well as the editor and reviewers for their comments that resulted in a greatly improved paper.

REFERENCES

Bracegirdle, T. J., and G. J. Marshall, 2012: The reliability of Antarctic tropospheric pressure and temperature in the latest global reanalyses. *J. Climate*, **25**, 7138–7146, doi:10.1175/JCLI-D-11-00685.1.

Bromwich, D. H., and R. L. Fogt, 2004: Strong trends in the skill of the ERA-40 and NCEP–NCAR reanalysis in the high and middle latitudes of the Southern Hemisphere, 1958–2001. *J. Climate*, **17**, 4603–4619, doi:10.1175/3241.1.

Ciasto, L. M., and D. W. J. Thompson, 2008: Observations of large-scale ocean atmosphere interaction in the Southern Hemisphere. *J. Climate*, **21**, 1244–1259, doi:10.1175/2007JCLI1809.1.

Clem, K. R., and R. L. Fogt, 2013: Varying roles of ENSO and SAM on the Antarctic Peninsula climate in austral spring. *J. Geophys. Res. Atmos.*, **118**, 11 481–11 492, doi:10.1002/jgrd.50860.

Dee, D. P., and Coauthors, 2011: The ERA-Interim reanalysis: Configuration and performance of the data assimilation system. *Quart. J. Roy. Meteor. Soc.*, **137**, 553–597, doi:10.1002/qj.828.

Deser, C., and J. Wallace, 1990: Large-scale atmospheric circulation features of warm and cold episodes in the tropical Pacific. *J. Climate*, **3**, 1254–1281, doi:10.1175/1520-0442(1990)003<1254:LSACFO>2.0.CO;2.

Diaz, H. F., and V. Markgraf, 1992: *El Niño: Historical and Paleoclimatic Aspects of the Southern Oscillation*. Cambridge University Press, 476 pp.

Fogt, R. L., and D. H. Bromwich, 2006: Decadal variability of the ENSO teleconnection to the high-latitude South Pacific governed by coupling with the southern annular mode. *J. Climate*, **19**, 979–997, doi:10.1175/JCLI3671.1.

——, ——, and K. M. Hines, 2011: Understanding the SAM influence on the South Pacific ENSO teleconnection. *Climate Dyn.*, **36**, 1555–1576, doi:10.1007/s00382-010-0905-0.

Folland, C. K., J. A. Renwick, M. J. Salinger, and A. B. Mullan, 2002: Relative influences of the Interdecadal Pacific Oscillation and ENSO on the South Pacific Convergence Zone. *Geophys. Res. Lett.*, **29**, doi:10.1029/2001GL014201.

Frauen, C., D. Dommenget, N. Tyrrell, M. Rezny, and S. Wales, 2014: Analysis of the nonlinearity of El Niño–Southern Oscillation teleconnections. *J. Climate*, **27**, 6225–6244, doi:10.1175/JCLI-D-13-00757.1.

Harangozo, S. A., 2000: A search for ENSO teleconnections in the west Antarctic Peninsula climate in Austral winter. *Int. J. Climatol.*, **20**, 663–679, doi:10.1002/(SICI)1097-0088(200005)20:6<663::AID-JOC493>3.0.CO;2-I.

Held, I. M., S. W. Lyons, and S. Nigam, 1989: Transients and the extratropical response to El Niño. *J. Atmos. Sci.*, **46**, 163–174, doi:10.1175/1520-0469(1989)046<0163:TATERT>2.0.CO;2.

Hoskins, B. J., and D. J. Karoly, 1981: The steady linear response of a spherical atmosphere to thermal and orographic forcing. *J. Atmos. Sci.*, **38**, 1179–1196, doi:10.1175/1520-0469(1981)038<1179:TSLROA>2.0.CO;2.

Houseago-Stokes, R. E., and G. R. McGregor, 2000: Spatial and temporal patterns linking southern low and high latitudes during South Pacific warm and cold events. *Int. J. Climatol.*, **20**, 793–801, doi:10.1002/1097-0088(20000615)20:7<793::AID-JOC502>3.0.CO;2-9.

Itterly, K. F., and P. C. Taylor, 2014: Evaluation of the tropical TOA flux diurnal cycle in MERRA and ERA-Interim retrospective analyses. *J. Climate*, **27**, 4781–4796, doi:10.1175/JCLI-D-13-00737.1.

Jin, D., and B. P. Kirtman, 2009: Why the Southern Hemisphere ENSO responses lead ENSO. *J. Geophys. Res.*, **114**, D23101, doi:10.1029/2009JD012657.

——, and ——, 2010: How the annual cycle affects the extratropical response to ENSO. *J. Geophys. Res.*, **115**, D06102, doi:10.1029/2009JD012660.

Jones, P. D., and D. H. Lister, 2015: Antarctic near-surface air temperatures compared with ERA-Interim values since 1979. *Int. J. Climatol.*, **35**, 1354–1366, doi:10.1002/joc.4061.

Karoly, D. J., 1989: Southern Hemisphere circulation features associated with El Niño–Southern Oscillation events. *J. Climate*, **2**, 1239–1252, doi:10.1175/1520-0442(1989)002<1239:SHCFAW>2.0.CO;2.

Lachlan-Cope, T., and W. Connolley, 2006: Teleconnections between the tropical Pacific and the Amundsen–Bellinghausens Sea: Role of the El Niño/Southern Oscillation. *J. Geophys. Res.*, **111**, D23101, doi:10.1029/2005JD006386.

Lazzara, M. A., G. A. Weidner, L. M. Keller, J. E. Thom, and J. J. Cassano, 2012: Antarctic Automatic Weather Station Program: 30 years of polar observations. *Bull. Amer. Meteor. Soc.*, **93**, 1519–1537, doi:10.1175/BAMS-D-11-00015.1.

L'Heureux, M. L., and D. W. J. Thompson, 2006: Observed relationships between the El Niño/Southern Oscillation and the extratropical zonal-mean circulation. *J. Climate*, **19**, 276–287, doi:10.1175/JCLI3617.1.

Li, X., E. P. Gerber, D. M. Holland, and C. Yoo, 2015: A Rossby wave bridge from the tropical Atlantic to West Antarctica. *J. Climate*, **28**, 2256–2273, doi:10.1175/JCLI-D-14-00450.1.

Marshall, G. J., 2003: Trends in the Southern Annular Mode from observations and reanalysis. *J. Climate*, **16**, 4134–4143, doi:10.1175/1520-0442(2003)016<4134:TITSAM>2.0.CO;2.

Mo, K. C., and G. H. White, 1985: Teleconnections in the Southern Hemisphere. *Mon. Wea. Rev.*, **113**, 22–37, doi:10.1175/1520-0493(1985)113<0022:TITSH>2.0.CO;2.

——, and W. Higgins, 1998: The Pacific–South American modes and tropical convection during the Southern Hemisphere winter. *Mon. Wea. Rev.*, **126**, 1581–1596, doi:10.1175/1520-0493(1998)126<1581:TPSAMA>2.0.CO;2.

NOAA/Climate Prediction Center, 2015: Oceanic Niño Index ERSST.v4b.NOAA/National Climatic Data Center, Subset used: January 1979–December 2013, accessed January 2015. [Available online at http://www.cpc.ncep.noaa.gov/products/analysis_monitoring/ensostuff/ensoyears_ERSSTv3b.shtml.]

Okumura, Y. M., and C. Deser, 2010: Asymmetry in the duration of El Niño and La Niña. *J. Climate*, **23**, 5826–5843, doi:10.1175/2010JCLI3592.1.

Philander, S. G., and E. M. Rasmusson, 1985: The southern oscillation and El Niño. *Advances in Geophysics*, Vol. 28, Academic Press, 197–215, doi:10.1016/S0065-2687(08)60224-1.

Schneider, D. P., Y. Okumura, and C. Deser, 2012: Observed Antarctic interannual climate variability and tropical linkages. *J. Climate*, **25**, 4048–4066, doi:10.1175/JCLI-D-11-00273.1.

Trenberth, K. E., 1975a: A quasi-biennial standing wave in the Southern Hemisphere and interrelations with sea surface temperature. *Quart. J. Roy. Meteor. Soc.*, **101**, 55–74, doi:10.1002/qj.49710142706.

——, 1975b: Reply to comment on 'A quasi-biennial standing wave in the Southern Hemisphere and interrelations with sea surface temperature' by K. E. Trenberth. *Quart. J. Roy. Meteor. Soc.*, **101**, 174–176.

——, 1976: Spatial and temporal variations of the southern oscillation. *Quart. J. Roy. Meteor. Soc.*, **102**, 639–653, doi:10.1002/qj.49710243310.

——, 1997: The definition of El Niño. *Bull. Amer. Meteor. Soc.*, **78**, 2771–2777, doi:10.1175/1520-0477(1997)078<2771:TDOENO>2.0.CO;2.

Turner, J., 2004: The El Niño–Southern Oscillation and Antarctica. *Int. J. Climatol.*, **24**, 1–31, doi:10.1002/joc.965.

Wilson, A. B., D. H. Bromwich, K. M. Hines, and S. Wang, 2014: El Niño flavors and their simulated impacts on atmospheric circulation in the high southern latitudes. *J. Climate*, **27**, 8934–8955, doi:10.1175/JCLI-D-14-00296.1.

Yu, L., Z. Zhang, M. Zhou, S. Zhong, D. Lenschow, H. Hsu, H. Wu, and B. Sun, 2010: Validation of ECMWF and NCEP-NCAR Reanalysis Data in Antarctica. *Adv. Atmos. Sci.*, **27**, 1151–1168, doi:10.1007/s00376-010-9140-1.